Photoionization Study of $(H_2S)_2$ and $(H_2S)_3$

H. F. Prest, W.-B. Tzeng, J. M. Brom, Jr.,† and C. Y. Ng*‡

Contribution from Ames Laboratory,§ U.S. Department of Energy, and Department of Chemistry, Iowa State University, Ames, Iowa 50011. *Received June 30, 1983*

Abstract: The internal energy effects and the energetics of the ion–molecule reactions $H_2S^+ + H_2S \rightarrow S_2^+ + 2H_2$, $HS_2^+ + H_2 + H$, $H_3S^+ + HS$, and $H_3S_2^+ + H$ have been studied by photoionization of hydrogen sulfide dimers synthesized by the molecular beam method. The appearance energy (AE) for H_3S^+ from $(H_2S)_2$ was determined to be 10.249 ± 0.012 eV (1209.7 ± 1.5 Å). This value allows the calculation of the absolute proton affinity for H_2S at 0 K to be 167.2 ± 1.4 kcal/mol. By use of the measured ionization energies for $(H_2S)_2^+$ (9.596 ± 0.022 eV) and $(H_2S)_3^+$ (9.467 ± 0.022 eV) and the estimated bonding energies for $H_2S{\cdot}H_2S$ and $(H_2S)_2{\cdot}H_2S$ (0.05 eV), the bond dissociation energies for $H_2S^+{\cdot}H_2S$ and $(H_2S)_2^+{\cdot}H_2S$ are deduced to be 0.92 ± 0.04 and 0.18 ± 0.04 eV, respectively. The AE for $H_3S^+{\cdot}H_2S$ from $(H_2S)_3$ (9.84 ± 0.04 eV) also makes possible the calculation of the bond dissociation energy for $H_3S^+{\cdot}H_2S$ to be 0.46 ± 0.10 eV.

The ion-molecule reactions between H_2S^+ and H_2S are relatively unexplored. Previous studies by high-pressure mass spectrometry,[1,2] selected ion flow tube,[3] and ion cyclotron resonance,[4-6] are in general agreement that the H_3S^+ ion is the most important product ion. The cyclotron ejection experiment of Huntress and Pinizzotto[6] showed that the formation of H_3S^+ proceeds almost equally via both proton transfer and hydrogen-atom abstraction. Their experiment further revealed that in addition to the $H_3S^+ + HS$ channel, charge transfer is also a major primary reaction channel for $H_2S^+ + H_2S$.

The S_2^+, HS_2^+, $H_2S_2^+$, and $H_3S_2^+$ ions, which were much lower in intensity in comparison with H_3S^+, have been observed by Ruska and Franklin[1] in a low-pressure ion source of H_2S. At higher source presures of H_2S, ions such as $H_5S_2^+$ and $H_2S_3^+$ resulting from condensation processes or termolecular mechanisms were also found. The results of a trapped ion study by Harrison[5] provided evidence that the S_2^+, HS_2^+, $H_2S_2^+$, and $H_3S_2^+$ ions were secondary in nature and were formed mainly by the reactions between S^+ and HS^+ with H_2S. The S^+ and HS^+ ions were among the major constituents in the ion source and were produced by electron impact ionization of H_2S. Nevertheless, the later experiment of Huntress and Pinizzotto has been able to identify HS_2^+ to be a primary product ion for the reaction of $H_2S^+ + H_2S$. These observations motivate us to search for the association of S_2^+, HS_2^+, $H_2S_2^+$, and $H_3S_2^+$ with the reactions between H_2S^+ and H_2S.

This report presents the results and an analysis of a study of the unimolecular decompositions of $(H_2S)_2^+$ and $(H_2S)_3^+$, which were prepared by photoionization of $(H_2S)_2$ and $(H_2S)_3$ formed in a supersonic beam of H_2S.

$$(H_2S)_2 + h\nu \rightarrow H_2S^+{\cdot}H_2S + e^- \rightarrow S_2^+ + 2H_2 + e^- \quad (1)$$

$$\rightarrow HS_2^+ + H_2 + H + e^- \quad (2)$$

$$\rightarrow H_2S_2^+ + H_2 + e^- \quad (3)$$

$$\rightarrow H_3S^+ + HS + e^- \quad (4)$$

$$\rightarrow H_3S_2^+ + H + e^- \quad (5)$$

$$(H_2S)_3 + h\nu \rightarrow H_2S^+{\cdot}(H_2S)_2 + e^- \rightarrow H_5S_2^+ + HS + e^- \quad (6)$$

By measuring the photoionization efficiency (PIE) spectra of S_2^+, HS_2^+, $H_2S_2^+$, H_3S^+, $H_3S_2^+$, and $(H_2S)_2^+$ from $(H_2S)_2$ and $H_5S_2^+$ and $(H_2S)_3^+$ from $(H_2S)_3$, we have been able to examine the internal energy effects and the energetics of reactions 1–6. The study of these unimolecular reactions is expected to have direct bearing on the formation of S_2^+, HS_2^+, $H_2S_2^+$, H_3S^+, and $H_3S_2^+$ from the reactions of $H_2S^+ + H_2S$ by the collisional complex mechanism. Similar photoionization studies on other systems[7-11] have been reported. The merits of the photoionization of van der Waals clusters have also been discussed previously.

Experimental Section

The experimental arrangement and procedures were essentially the same as those described previously.[12,13] Briefly, the apparatus consists of a 3-m near-normal incidence vacuum ultraviolet (VUV) monochromator (McPherson 2253M), a supersonic molecular beam production system, a capillary discharge lamp, a VUV light detector, and a quadrupole mass spectrometer for ion detection. The grating employed in this study was a Bausch & Lomb 1200 lines/mm MgF_2-coated aluminum grating blazed at 1360 Å. Either the hydrogen many-lined pseudocontinuum or the helium Hopfield continuum was used as the light source, depending on the wavelength region desired.

The hydrogen sulfide was obtained from Matheson with a quoted purity of ≥99.6%. The H_2S molecular beam was produced by supersonic expansion through a 120 μm diameter (D) stainless steel nozzle. The nozzle stagnation pressure (P_0) was varied in the range of ~150–500 torr. With the exception of the PIE spectrum of H_2S^+,[14] which was obtained at a nozzle temperature (T_0) of 290 K, all the other PIE spectra were measured at $T_0 \approx 230$ K. In a typical run, the fluctuation in the nozzle temperature was less than ±3 K as monitored with thermocouples. Since the hydrogen sulfide beam was sampled in a collisionless environment, the observed fragment ions represent the primary fragments of H_2S^+, $(H_2S)_2^+$, $(H_2S)_3^+$, and higher hydrogen sulfide cluster ions.

All the data were obtained with an optical resolution of 1.4 Å (FWHM). Data points were taken typically at either 0.5- or 1-Å intervals. The standard deviations of PIE data presented here are better than 10%. Each PIE spectrum was based on at least two scans, and prominent structures in the curves were found to be reproducible. Wavelength calibrations were achieved by using known atomic resonance lines or H_2 emission lines[15] when the H_2 pseudocontinuum was used.

† Present address: Department of Chemistry, Benedictine College, Atchison, Kansas 66002.

‡ Alfred P. Sloan Research Fellow. Camille and Henry Dreyfus Teacher-Scholar.

§ Operated for the U.S. Department of Energy by Iowa State University under Contract No. W-7405-Eng-82. This work was supported by the Director of Energy Research, Office of Basic Energy Science.

(1) W. E. W. Ruska and J. L. Franklin, *Int. J. Mass Spectrom. Ion Phys.*, **3**, 221 (1969).
(2) S. K. Gupta, E. G. Jones, A. G. Harrison, and J. J. Myher, *Can. J. Chem.*, **45**, 3107 (1967).
(3) D. Smith, N. G. Adams, and W. Lindinger, *J. Chem. Phys.*, **75**, 3365 (1981).
(4) J. L. Beauchamp and S. E. Buttrill, Jr., *J. Chem. Phys.*, **48**, 1783 (1967).
(5) A. G. Harrison, *Int. J. Mass Spectrom. Ion Phys.*, 6, 297 (1971).
(6) W. T. Huntress, Jr., and R. F. Pinizzato, Jr., *J. Chem. Phys.*, **59**, 4742 (1973).
(7) Y. Ono, S. H. Linn, H. F. Prest, M. E. Gress, and C. Y. Ng. *J. Chem. Phys.*, **74**, 1125 (1981).
(8) S. T. Ceyer, P. W. Tiedemann, C. Y. Ng, B. H. Mahan, and C. Y. Ng, *J. Chem. Phys.*, **70**, 2138 (1979).
(9) Y. Ono and C. Y. Ng, *J. Chem. Phys.*, **77**, 2947 (1982).
(10) Y. Ono and C. Y. Ng, *J. Am. Chem. Soc.*, **104**, 4752 (1982).
(11) C. Y. Ng, *Adv. Chem. Phys.*, **52**, 263 (1983).
(12) Y. Ono, S. H. Linn, H. F. Prest, M. E. Gress, and C. Y. Ng, *J. Chem. Phys.*, **73**, 2523 (1980).
(13) Y. Ono, S. H. Linn, H. F. Prest, C. Y. Ng, and E. Meischer, *J. Chem. Phys.*, **73**, 4855 (1980).
(14) H. F. Prest, W.-B. Tzeng, J. M. Brom, Jr., and C. Y. Ng, *Int. J. Mass Spectrom. Ion Phys.*, **50**, 315 (1983). V. H. Dibeler and S. K. Liston, *J. Chem. Phys.*, **49**, 482 (1968).

0002-7863/83/1505-7531$01.50/0

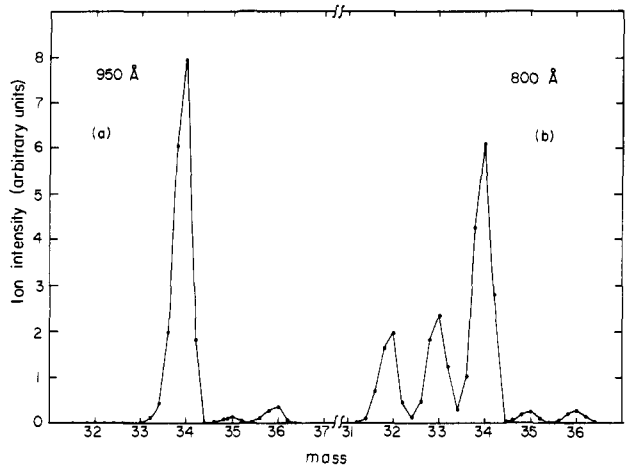

Figure 1. Mass spectra of H_2S obtained at (a) 950 and (b) 800 Å.

Stemming from the fact that the ions of interest in this experiment, S_2^+, HS_2^+, $H_2S_2^+$, H_3S^+, $H_3S_2^+$, and $H_5S_2^+$, were, in general, much lower in intensity in comparison with the intensities of S^+, HS^+, H_2S^+, $(H_2S)_2^+$, and $(H_2S)_3^+$, it was necessary to operate the mass spectrometer at a resolution sufficiently high to minimize the contribution of intense ions to weaker fragments. The major isotopes of sulfur are ^{32}S, ^{33}S, and ^{34}S, which have the natural abundances of 95, 0.76, and 4.22%,[16] respectively. Maintaining a high mass resolution also makes possible a meaningful correction of the sulfur and hydrogen isotopic effects. The mass spectra of H_2S in the mass range m/e = 31–36 obtained at 950 and 800 Å are shown in parts a and b of Figure 1, respectively, to illustrate the typical mass resolution used in this study.

Results and Discussion

Figure 2b shows the PIE curve for $(H_2S)_2^+$ in the region 640–1310 Å obtained at $P_0 \approx 465$ torr. The PIE spectrum for H_2S^+, measured with the same optical resolution, is shown in Figure 2a for comparison. The analyses of the PIE spectra for H_2S^+ and its fragment ions S^+ and HS^+ have been reported previously.[14] The general profile of the PIE curve for $(H_2S)_2^+$ is similar to that for H_2S^+ in the region ~927–1185 Å. In accordance with the observations in other systems,[9,17-20] autoionizing structures resolved in the H_2S^+ spectrum are hardly discernible in the $(H_2S)_2^+$ spectrum. Since autoionizing Rydberg states in this region have mostly been assigned as vibrationally excited states,[14] the lack of structures in the PIE curve for $(H_2S)_2^+$ is likely due to efficient vibrational predissociation of excited Rydberg states of the hydrogen sulfide dimers.

At ~927 Å, the PIE for H_2S^+ starts to decrease toward higher photon energies, whereas the PIE for $(H_2S)_2^+$ continues to increase gradually until ~780 Å. The decrease in PIE for H_2S^+ is a consequence of strong predissociations of H_2S^+ to form S^+ and HS^+ in this region.[14]

$$H_2S^+ \rightarrow S^+ + H_2 \quad (7)$$

$$\rightarrow HS^+ + H \quad (8)$$

After including the PIEs for S^+ and HS^+, the corrected PIE curve for H_2S^+ in the region ~780–927 Å (the upper curve in Figure 2a) is found to roughly resemble the shape of the PIE curve for $(H_2S)_2^+$. This observation can be taken as evidence that the probabilities for dissociation processes of $(H_2S)_2^+$ such as

$$H_2S^+\cdot H_2S \rightarrow S^+\cdot H_2S + H_2 \quad (9)$$

$$\rightarrow HS^+\cdot H_2S + H \quad (10)$$

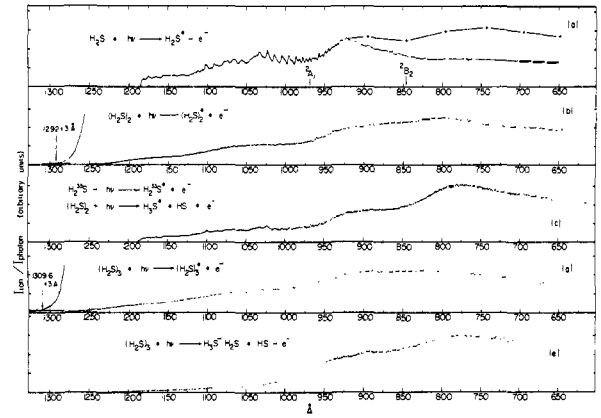

Figure 2. (a) PIE curve for H_2S^+ in the region 650–1185 Å (nozzle conditions: $P_0 \approx 150$ torr; $T_0 \approx 298$ K; $D = 120$ μm). (b) PIE curve for $(H_2S)_2^+$ in the region 640–1310 Å (nozzle conditions: $P_0 \approx 465$ torr; $T_0 \approx 230$ K; D = 120 μm). (c) PIE curve for the mass 35 ions ($H_3{}^{32}S^+ + H_2{}^{33}S^+ + H^{34}S^+$) in the region 600–1185 Å (nozzle conditions: $P_0 \approx 465$ torr; $T_0 \approx 230$ K; $D = 120$ μm). (d) PIE curve for $(H_2S)_3^+$ in the region 650–1325 Å (nozzle conditions: $P_0 \approx 465$ torr; $T_0 \approx 230$ K; $D = 120$ μm). (e) PIE curve for the mass 69 ions ($H_3{}^{32}S^+\cdot H_2{}^{32}S + H_2{}^{32}S^+\cdot H_2{}^{33}S + H_2{}^{33}S^+\cdot H_2{}^{32}S + H^{34}S^+\cdot H_2{}^{32}S^+ + H^{32}S^+\cdot H_2{}^{34}S$) in the region 700–1300 Å (nozzle conditions: $P_0 \approx 500$ torr; $T_0 \approx 230$ K; $D = 120$ μm). All PIE spectra were obtained with a wavelength resolution of 1.4 Å (FWHM).

are much lower than those of the corresponding reactions 7 and 8. In view of the fact that the $H_2S^+\cdot H_2S$ complex has more degrees of freedom in which to redistribute the excess energy of the H_2S^+ moiety in the dimer ion, according to statistical theory, it is reasonable to expect that reactions 9 and 10 are less favorable in comparison with reactions 7 and 8 for the same amount of excess energy. The decreasing trend found in the PIE curve for $(H_2S)_2^+$ in the region ~650–800 Å correlates well with the corresponding increases in the formation of S_2^+, HS_2^+, $H_2S_2^+$, H_3S^+, and $H_3S_2^+$ via reactions 1–5, which will be discussed in later sections.

The ionization energy (IE) for $(H_2S)_2^+$ determined in this study was 9.596 ± 0.022 eV (1292 ± 3 Å), which is 0.14 eV lower in energy than that reported recently by Walters and Blais.[21] The existence of weak hydrogen bonding between H_2S molecules was concluded by Harada and Kitamura[22] from considerations based on the structure of solid hydrogen sulfide. From second virial coefficient data,[23,24] the well depth for H_2S–H_2S interaction can be estimated to be 0.028 eV. In a spectroscopic study, Lowder et al.[25] obtained a dimerization energy of 0.074 ± 0.013 eV for $(H_2S)_2$. Depending on the geometry of the H_2S dimer, theoretical calculations yielded values in the range 0.01–0.08 eV.[26-29] Here, the average experimental value 0.05 ± 0.03 eV is used as the bond dissociation energy (D_0) for $H_2S\cdot H_2S$. When the IEs of H_2S (10.4607 ± 0.0026 eV)[14,30,31] and $(H_2S)_2$ and the value for $D_0[(H_2S)_2]$ are used, $D_0[(H_2S)_2^+]$ can be calculated from the relation

$$D_0[(H_2S)_2^+] = IE(H_2S) + D_0[(H_2S)_2] - IE[(H_2S)_2] \quad (11)$$

The calculated value for $D_0[(H_2S_2)_2^+]$ is 0.92 ± 0.04 eV (21.2

(15) K. E. Schubert and R. D. Hudson, "A Photoelectric Atlas of the Intense Lines of the Hydrogen Molecular Emission Spectrum from 1025 to 1650 Å at a Resolution of 0.1 Å", Aerospace Corp., Los Angeles, 1963, Report No. ATN-64(9233)-2.
(16) G. Friedlander, J. W. Kennedy, and J. M. Miller, "Nuclear and Radiochemistry", Wiley, New York, 1964, Appendix E.
(17) S. H. Anderson, T. Hirooka, P. W. Tiedemann, B. H. Mahan, and Y. T. Lee, *J. Chem. Phys.*, **73**, 4779 (1980).
(18) S. H. Linn, Y. Ono, and C. Y. Ng, *J. Chem. Phys.*, **74**, 3348 (1981).
(19) S. H. Linn, Y. Ono, and C. Y. Ng, *J. Chem. Phys.*, **74**, 3342 (1981).
(20) S. H. Linn and C. Y. Ng, *J. Chem. Phys.*, **75**, 4921 (1981).
(21) E. A. Walters and N. C. Blais, *J. Chem. Phys.*, **75**, 4208 (1981).
(22) J. Harada and N. Kitamura, *J. Phys. Soc. Jpn.*, **19**, 328 (1964).
(23) F. Khoury and D. B. Robinson, *J. Chem. Phys.*, **55**, 834 (1971).
(24) P. Seal and P. K. Bandyopadhyay, *Indian J. Phys.*, **48**, 684 (1974).
(25) J. E. Lowder, L. A. Kennedy, K. G. P. Sulzmann, and S. S. Penner, *J. Quantum Spectrosc.*, **10**, 17 (1970).
(26) R. C. Kerns and L. C. Allen, *J. Am. Chem. Soc.*, **100**, 6587 (1978).
(27) J. R. Sabin, *J. Am. Chem. Soc.*, **93**, 3613 (1971).
(28) G. Leroy, G. Louterman-Leloup, and P. Ruelle, *Bull. Soc. Chim. Belg.*, **85**, (4), 219 (1976).
(29) B. van Hensbergen, R. Block, and L. Jansen, *J. Chem. Phys.*, **76**, 3161 (1982).
(30) L. Karlsson, L. Mattsson, R. Jadrny, T. Bergmark, and K. Siegbahn, *Phys. Scr.*, **13**, 229 (1976).
(31) H. Masuko, Y. Morioka, M. Nakamura, E. Ishiguro, and M. Sasanuma, *Can. J. Phys.*, **57**, 745 (1979).
(32) C. Y. Ng, D. J. Trevor, P. W. Tiedemann, S. T. Ceyer, P. L. Kronebush, B. H. Mahan, and Y. T. Lee, *J. Chem. Phys.*, **67**, 4235 (1977).

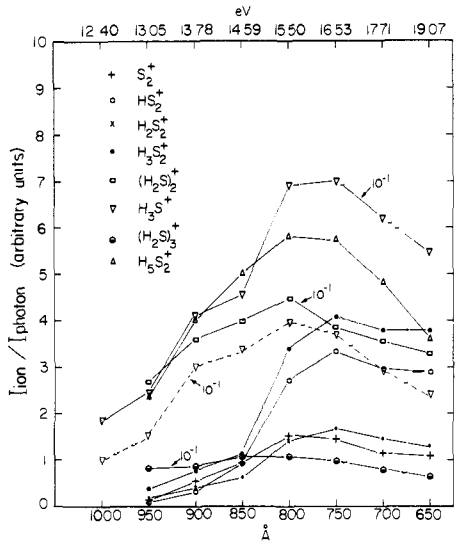

Figure 3. The Relative PIEs for $(H_2S)_3^+$, $H_5S_2^+$, $(H_2S)_2^+$, $H_3S_2^+$, $H_2S_2^+$, HS_2^+, S_2^+, and H_3S^+ in the region ~650–1000 Å obtained with $P_0 \approx$ 360 torr and $T_0 \approx 230$ K. The PIE spectra connected by solid lines have not been corrected for isotopic effects. The PIE spectrum for H_3S^+ connected by dashed lines has been corrected for isotopic contributions. No corrections were made to account for transmission factors of these ions through the mass spectrometer used in this experiment.

± 0.9 kcal/mol). This value is comparable to the bond dissociation energies of many other simple inorganic and organic dimer ions,[9,10,12,18,19,33,34] but substantially lower than the value of 1.58 ± 0.13 eV for $D_0[(H_2O)_2^+]$.[32,35]

The PIE data for $(H_2S)_3^+$ in the region ~650–1325 Å obtained at $P_0 \approx$ 460 torr are plotted in Figure 2d. The PIE curves for $(H_2S)_3^+$ and $(H_2S)_2^+$ are similar in appearance. The IE of $(H_2S)_3$ was determined to be 9.467 ± 0.022 eV (1309.6 ± 3 Å), which is also found to be lower than a value of 9.63 ± 0.01 eV obtained by Walters and Blais.[21] Assuming that the bond dissociation energy for $(H_2S)_2 \cdot H_2S$ is the same as that for $H_2S \cdot H_2S$ and when the IEs of $(H_2S)_2$ and $(H_2S)_3$ are used, a value of 0.18 ± 0.04 eV for $D_0[(H_2S)_2^+ \cdot H_2S]$ is deduced from a relation similar to eq 11.

The PIE spectrum for the mass 35 ions in the region ~600–1200 Å is shown in Figure 2c. The $H_3{}^{32}S^+$, $H_2{}^{33}S^+$, $H^{34}S^+$, $DH^{32}S^+$, and $D^{33}S^+$ ions cannot be resolved by our quadrupole mass spectrometer. Considering the low natural abundance of the deuterium isotope (0.015%),[16] the intensities of the latter two ions should be much lower than those of $H_3{}^{32}S^+$, $H_2{}^{33}S^+$, and $H^{34}S^+$. In the region ~925–1200 Å, the spectrum of the mass 35 ions exhibits the same structure observed in the PIE curve for H_2S^+, an observation indicating that the mass 35 ions in this region are predominately the $H_2{}^{33}S^+$ ions formed by the direct photoionization of H_2S. The profiles of the PIE curves for the mass 35 ions and $(H_2S)_2^+$ are similar in the region ~850–925 Å. At wavelengths shorter than ~867 Å, which is the AE for the formation of HS^+ from H_2S,[14] we find that the $H^{34}S^+$ ions are mainly responsible for the further increase in PIE of the mass 35 ions. In principle, the true PIE curve for $H_3{}^{32}S^+$ can be obtained by substracting the intensities of $H_2{}^{33}S^+$ and $H^{34}S^+$ from that of the mass 35 ions. The true and the uncorrected PIE curves for H_3S^+ in the region ~650–1000 Å are compared in Figure 3. The profile for the true PIE curve for H_3S^+ is again found to bear some resemblance to that for $(H_2S)_2^+$. The true PIE for H_3S^+ decreases dramatically from ~925 Å toward longer wavelengths. In the region ~950–1180 Å, the intensity of H_3S^+ is less than 10% that of the $H_2{}^{33}S^+$ ion.

Table I. Heats of Formation at 0 K in kcal/mol of Neutrals and Ions[a]

compound	neutrals	ions
$(H_2S)_3$	−14.9 ± 1.0 (36)	203.5 ± 1.1[b]
$H_5S_2^+$		178.9 ± 1.8[b]
$(H_2S)_2$	−9.4 ± 0.7 (36)	211.9 ± 0.9[b]
$H_3S_2^+$		<238[b]
$H_2S_2^+$		239–246[c] (37)
		<290[b]
HS_2^+		232–249[c] (6)
		<248[b]
S_2^+		~246[b]
H_3S^+		193.8 ± 1.4[b]
		188.3–193.3[c] (36, 39, 40)
H_2S	−4.2 ± 0.2 (40)	237.02 ± 0.21 (14, 38)
	−4.9 ± 0.2 (40)	
HS	33.14 ± 1.2 (40)	~274 (38)
	33.3 ± 1.2[c] (40)	
S	65.66 ± 0.06 (40)	305 (38)
	66.20 ± 0.06[c] (40)	
H	51.631 ± 0.001 (36)	365.236 ± 0.01 (36)
	52.100 ± 0.001[c] (36)	367.186 ± 0.01 (36)

[a] The numbers in parentheses are the references. [b] This work. Because of the high degree of rotational and low-frequency vibrational relaxation in the supersonic expansion, these values can be considered to be the heats of formation at 0 K. [c] Heats of formation at 298 K.

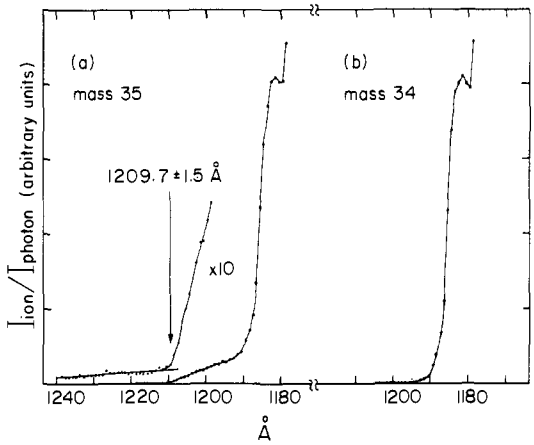

Figure 4. PIE curves for (a) the mass 35 ions ($H_2{}^{33}S^+ + H_3{}^{32}S^+$) and (b) the mass 34 ion ($H_2{}^{32}S^+$) in the region ~1178–1240 Å obtained with a wavelength resolution of 1.4 Å (FWHM). The PIEs for the mass 34 and 35 ions have been normalized at 1180 Å (nozzle conditions: $P_0 \approx$ torr; $T_0 \approx 230$ K).

According to thermodynamical data listed in Table I,[36–40] the AE for reaction 4 is predicted to be in the range ~10.07–10.29 eV (1231–1205 Å), which is slightly lower than the IE of H_2S. Since one anticipates that the PIE spectra for $H_2{}^{33}S^+$ and $H_2{}^{32}S^+$ are identcial and that the $H_2{}^{33}S^+$ ions cannot be formed below the IE of H_2S, a careful examination of the PIE curves for the mass 35 ($H_2{}^{33}S^+ + H_3{}^{32}S^+$) and the mass 34 ($H_2{}^{32}S^+$) ions below the ionization threshold for H_2S should make possible the identification of the PIE curve for H_3S^+. Parts a and b of Figure 4

(33) Y. Ono, E. A. Osuch, and C. Y. Ng, *J. Chem. Phys.*, **74**, 1645 (1981).
(34) J. Erickson and C. Y. Ng, *J. Chem. Phys.*, **75**, 1650 (1981).
(35) S. Tomoda, Y. Achiba, and K. Kimura, *Chem. Phys. Lett.*, **87**, 197 (1982).
(36) JANAF Thermochemical Tables, *Natl. Stand. Ref. Data Ser.* (*U.S., Natl. Bur. Stand.*), **37**, (1971).
(37) J. L. Franklin, J. G. Dillard, H. M. Rosenstock, J. T. Herron, K. Draxl, and F. H. Field, *Natl. Stand. Ref. Data Ser.*, (*U.S., Natl. Bur. Stand.*), **26** (1969).
(38) H. M. Rosenstock, K. Draxl, B. W. Steiner, and J. T. Herron, *J. Phys. Chem. Ref. Data Suppl.*, **6** (1977).
(39) R. Walder and J. L. Franklin, *Int. J. Mass Spectrom. Ion Phys.*, **36**, 85 (1980).
(40) D. S. Marynick, K. Scanlon, R. A. Eades, and D. A. Dixon, *J. Phys. Chem.*, **85**, 3364 (1981).
(41) M. W. Chase, Jr., J. L. Curnutt, J. R. Downey, Jr., R. A. McDonald, A. N. Syverud, and E. A. Valenzuela, *J. Phys. Chem. Ref. Data* **11**, 695 (1982).

show the PIE curves in the region ~1180–1240 Å for the mass 35 and 34 ions, respectively. The PIEs for the mass 34 and 35 ions were normalized at 1180 Å. As expected, this comparison clearly brings out the difference between the PIE spectra for the mass 34 and 35 ions in the energy range lower than the IE of H_2S. The finite yields observed for the mass 35 ions in the region ~1190–1210 Å are definitely due to reaction 4. The AE for the formation of H_3S^+ is quite distinct and has a value of 10.249 ± 0.012 eV (1209.7 ± 1.5 Å). From the latter value, together with the known heats of formation for $(H_2S)_2$[36] and HS[40] at 0 K (Table I), the heat of formation for H_3S^+ at 0 K is calculated to be 193.8 ± 1.4 kcal/mol. The proton affinity is equal to the enthalpy change for the reaction

$$H_2S + H^+ \rightarrow H_3S^+ \quad (12)$$

When the value for $\Delta H°_{f0}(H_3S^+)$ and the values for $\Delta H°_{f0}(H_2S)$[40] and $\Delta H°_{f0}(H^+)$[36] (Table I) are used, the absolute proton affinity for H_2S at 0 K is deduced to be 167.2 ± 1.4 kcal/mol. We note that the uncertainty of the proton affinity determined here is largely due to the uncertainties in $\Delta H°_{f0}(HS)$ and to a smaller extent due to the bond dissociation energy of $H_2S{\cdot}H_2S$. Conventionally, the proton affinity is referred to 298 K. Assuming an ideal gas model and excluding any vibrational and electronic contributions to the heat capacities of H_2S and H_3S^+, a value of 168.7 ± 1.4 kcal/mol can be obtained for the absolute proton affinity of H_2S at 298 K. The latter value is found to be in agreement with the literature values.[42-47]

The PIE curve for the mass 69 ions in the region ~700–1300 Å is shown in Figure 2e. The mass 69 ions observed here mainly consist of the $H_5{}^{32}S_2{}^+$, $H_2{}^{32}S^+{\cdot}H_2{}^{33}S$, $H_2{}^{33}S^+{\cdot}H_2{}^{32}S$, $H^{34}S^+{\cdot}H_2{}^{32}S$, and $H^{32}S^+{\cdot}H_2{}^{34}S$ ions. Similarity in appearance can be found between the PIE curves for the mass 35 and the mass 69 ions in the region ~700–925 Å. The contributions attributable to the $H^{34}S^+{\cdot}H_2{}^{32}S^+$ and $H^{32}S^+{\cdot}H_2{}^{34}S$ ions to the intensity of the mass 69 ions observed here in the region ~700–870 Å are much lower than the corresponding contribution of the $H^{34}S^+$ ion to the observed intensity of the mass 35 ions. This is consistent with the conclusion that the intensity of the $HS^+{\cdot}H_2S$ ions formed by fragmentations of hydrogen sulfide dimers and clusters is much lower than that of HS^+ from H_2S. At photon wavelengths longer than ~890 Å, the contributions of the $H^{34}S^+{\cdot}H_2{}^{32}S$ and $H^{32}S^+{\cdot}H_2{}^{34}S$ ions become negligible in comparison with those of $H_5{}^{32}S_2{}^+$, $H_2{}^{32}S^+{\cdot}H_2{}^{33}S$, and $H_2{}^{33}S^+{\cdot}H_2{}^{32}S$. The ratio of the intensity of $H_5{}^{32}S_2{}^+$ to that of $H_2{}^{32}S^+{\cdot}H_2{}^{33}S + H_2{}^{33}S^+{\cdot}H_2{}^{32}S$ is approximately 0.9 at 1190 Å. At 1250 Å, this ratio decreases to ~0.2. After a careful correction for the contributions from the $H_2{}^{32}S^+{\cdot}H_2{}^{33}S$ and $H_2{}^{33}S^+{\cdot}H_2{}^{32}S$ ions, the AE for the formation of $H_3S^+{\cdot}H_2S$ by reaction 6 is determined to be 1260 ± 5 Å (9.84 ± 0.04 eV). By use of the latter value and the known heats of formation for $(H_2S)_3$ and HS at 0 K (Table I), $\Delta H°_{f0}(H_5S_2^+)$ is calculated to be 178.9 ± 1.9 kcal/mol. The latter value and $\Delta H°_{f0}(H_3S^+)$ determined here allow a value of 10.7 ± 2.2 kcal/mol to be calculated for the enthalpy change of the association reaction at 0 K.

$$H_3S^+ + H_2S \rightarrow H_3S^+{\cdot}H_2S \quad (13)$$

In a study by pulsed, high-pressure mass spectrometry, Meot-Ner and Field[48] obtained a value of 12.8 ± 1.5 kcal/mol for the enthalpy change of reaction 13 at approximately 370 K. Assuming an ideal-gas model and excluding any vibrational and electronic contributions to the heat capacities of H_3S^+, H_2S, and $H_3S^+{\cdot}H_2S$, it can be shown that the latter value corresponds to a value of 10.6 ± 1.5 kcal/mol for $\Delta H°_0$, which is in excellent agreement with the value derived from this study.

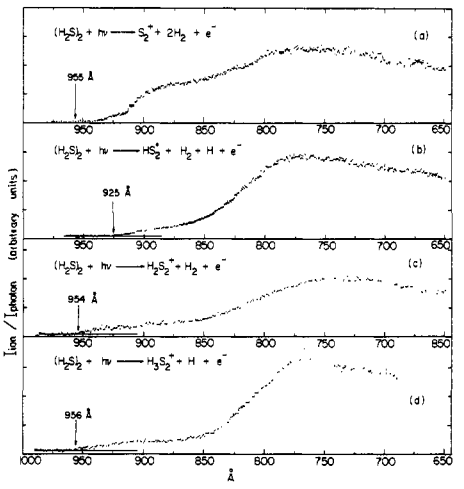

Figure 5. PIE curves for (a) S_2^+, (b) HS_2^+, (c) $H_2S_2^+$, and (d) $H_3S_2^+$ in the region ~650–1000 Å obtained with a wavelength resolution of 1.4 Å (FWHM) (nozzle conditions: $P_0 \approx 360$ torr; $T_0 \approx 230$ K).

The realtive PIEs for $(H_2S)_3^+$, $H_5S_2^+$, $(H_2S)_2^+$, $H_3S_2^+$, $H_2S_2^+$, HS_2^+, S_2^+, and H_3S^+ in the region 650–1000 Å obtained with $P_0 \approx 360$ torr and $T_0 \approx 230$ K are plotted in Figure 3 at intervals of 50 Å. Although the PIEs of these ions have not been corrected for isotopic contributions, these measurements show that S_2^+, HS_2^+, $H_2S_2^+$, and $H_3S_2^+$ are minor fragment ions from the hydrogen sulfide dimer and cluster ions. In the nozzle expansion conditions used here, the hydrogen sulfide dimers and trimers are the dominate cluster species in the beam. At $T_0 \approx 230$ K, the relative intensities of these ions measured at a given wavelength were found to be strongly dependent upon P_0, which in effect determines the distribution in concentration of the hydrogen sulfide clusters in the beam. This observation is consistent with the interpretation that not only can the S_2^+, $H_2S_2^+$, HS_2^+, $H_3S_2^+$, and H_3S^+ ions be formed by reactions 1–5 but also they can be produced by fragmentations of higher cluster ions such as $(H_2S)_3^+$.

$$(H_2S)_3 + h\nu \rightarrow (H_2S)_3^+ + e^- \rightarrow S_2^+ + H_2S + 2H_2 + e^- \quad (14)$$

$$\rightarrow HS_2^+ + H_2S + H_2 + H + e^- \quad (15)$$

$$\rightarrow H_2S_2^+ + H_2S + H_2 + e^- \quad (16)$$

$$\rightarrow H_3S_2^+ + H_2S + H + e^- \quad (17)$$

$$\rightarrow H_3S^+ + H_2S + HS + e^- \quad (18)$$

Nevertheless, the PIE curves for S_2^+, HS_2^+, $H_2S_2^+$, and $H_3S_2^+$ were found to be quite insensitive to changes in P_0 at $T_0 \approx 230$ K in the range of $P_0 \approx 200$–460 torr. Stemming from the expectation that the AEs of the above reactions are higher than those for the corresponding reactions 1–5, the existence of $(H_2S)_3$ and higher hydrogen sulfide clusters in the beam should not affect the AE measurements for fragment ions from $(H_2S)_2$. The finding that the AE for H_3S^+ is in accordance with the expected thermochemical value for reaction 4 can be taken as evidence in support of the above expectation.

The PIE curves for S_2^+, HS_2^+, $H_2S_2^+$, and $H_3S_2^+$ (uncorrected for isotopic contributions) in the region ~650–1000 Å obtained with $P_0 \approx 350$ torr and $T_0 \approx 230$ K are shown in parts a, b, c, and d of Figure 5, respectively. Other than the spectrum for S_2^+, the PIE curves for HS_2^+ $H_2S_2^+$, and $H_3S_2^+$ all suffered from the sulfur isotopic effects. However, because the intensities for the S_2^+, HS_2^+, $H_2S_2^+$, and $H_3S_2^+$ ions are similar and the natural abundances for ^{33}S and ^{34}S are small, the corrections due to isotopic contributions should only introduce minor modifications of the spectra.

The PIE curve shown in Figure 5a represents the true PIE spectrum for S_2^+. Within the sensitivity of our apparatus, an upperbound for the AE for S_2^+ was determined to be 12.98 eV (955 Å). On the basis of the known values for $\Delta H°_{f0}(S_2^+)$[38] and

(42) M. A. Haney and J. L. Franklin, *J. Chem. Phys.*, **50**, 2028 (1969).
(43) J. L. Beauchamp and S. K. Butrill, *J. Chem. Phys.*, **48**, 1783 (1968).
(44) K. Tanaka, G. I. Mackay, and D. K. Bohme, *Can. J. Chem.*, **56**, 193 (1978).
(45) L. Y. Wei and L. I. Bone, *J. Phys. Chem.*, **78**, 2527 (1974).
(46) J. M. Hopkins and L. I. Bone, *J. Chem. Phys.*, **58**, 1473 (1973).
(47) A comparison of values for the proton affinity of H_2S reported previously can be found in ref 39.
(48) M. Meot-Ner and F. H. Field, *J. Am. Chem. Soc.*, **99**, 998 (1977).

$\Delta H°_{f0}[(H_2S)_2]$ (Table I), the thermochemical threshold for the formation of $_2^+$ by reaction 1 is predicted to be 11.07 eV (1120 Å). The difference of 1.91 eV (44 kcal/mol) between the latter value and the experimental threshold can be taken to be an upper limit for the activation energy for the formation of $S_2^+ + 2H_2$ from the reaction of $H_2S^+ + H_2S$.

In the case of the PIE spectrum for HS_2^+ (Figure 5b), the isotopic contribution from the $^{32}S^{33}S^+$ ion near the threshold region (>900 Å) is more serious. After the contribution of $^{32}S^{33}S^+$ is accounted for, an upper bound for the AE for the formation of HS_2^+ by reaction 2 was estimated to be 13.40 eV (925 Å). The heat of formation for HS_2^+ is not known. By using the measured AE of HS_2^+ and thermochemical data for $(H_2S)_2$ and H,[36] the heat of formation for HS_2^+ is estimated to be 248 kcal/mol. The previous observations of the reactions $S^+ + H_2S \rightarrow HS_2^+ + H$ and $HS_2^+ + H_2O \rightarrow H_3O^+ + S_2$ have placed $\Delta H°_{f0}(HS_2^+)$ in the range of 232–249 kcal/mol.[6] Thus, the value for $\Delta H°_{f0}(HS_2^+)$ deduced here is consistent with these limits.

The intensity of the mass 66 ions, which is mostly due to $H_2{}^{32}S_2^+$, is comparable to that of S_2^+. After correction for minor contributions to the observed PIEs from $^{34}S^{32}S^+$ and $H^{33}S^{32}S^+$, an upperbound for the AE for reaction 3 is estimated to be 13.00 eV (954 Å). According to previous electron impact studies,[37] $\Delta H°_{f0}(H_2S_2^+)$ is in the range 239–246 kcal/mol. These limits imply the AE for $H_2S_2^+$ should be in the range ~10.77–11.08 eV (1119–1151 Å). The comparison between the latter value and the experimental AE for $H_2S_2^+$ places an upper limit of ~48 kcal/mol for the activation energy for the formation of $H_2S_2^+ + H_2$ from the reaction $H_2S^+ + H_2S$.

Since the intensity for $H_3S_2^+$ is greater than those for $H_2S_2^+$ and HS_2^+ in the region ~700–1000 Å (see Figure 3), the contributions from $H_2{}^{22}S^{33}S^+$ and $H^{32}S^{34}S^+$ to the PIE spectrum for $H_3S_2^+$ (Figure 5d) are minor. The AE for the formation of $H_3S_2^+$ from reaction 5 was found to be 12.97 eV (956 Å). The heat of formation of $H_3S_2^+$ has not been reported previously. The measured AE for $H_3S_2^+$ makes possible the calculation of a value of 238 kcal/mol for $\Delta H°_{f0}(H_3S_2^+)$. In view of the large activation energies observed for the formation of S_2^+ and $H_2S_2^+$ from reactions 1 and 3, respectively, the values for $\Delta H°_{f0}(HS_2^+)$ and $\Delta H°_{f0}(H_3S_2^+)$ derived from AE measurements here are likely to be upper limits.

The reactions of HS^+ and S^+ and H_2S have been observed

$$HS^+ + H_2S \rightarrow H_3S^+ + S \quad (19)$$

$$\rightarrow HS_2^+ + H_2 \quad (20)$$

$$\rightarrow H_2S_2^+ + H \quad (21)$$

$$S^+ + H_2S \rightarrow S_2^+ + H_2 \quad (22)$$

$$\rightarrow HS_2^+ + H \quad (23)$$

previously.[3,5,6] The AEs for the formations of S^+ and HS^+ from H_2S by photoionization have been reported to have the values of 13.37 eV (927 ± 1.5 Å) and 14.30 eV (867 ± 1.5 Å), respectively. The PIE spectra for S_2^+, HS_2^+, $H_2S_2^+$, $H_3S_2^+$, and H_3S^+ only show minor resemblance to the PIE spectra for S^+ and HS^+. On the basis of the observations that the AEs for S_2^+, HS_2^+, $H_2S_2^+$, and $H_3S_2^+$ are close to the AEs of S^+ and HS^+ and that the intensities of S^+ and HS^+ produced in this region are much higher than that of $(H_2S)_2^+$, it is reasonable to suspect that the S_2^+, HS_2^+, and $H_2S_2^+$ ions might have the origin from reactions 20–23. In order to examine the possible influence of these secondary reactions, the PIE curves for S_2^+, HS_2^+, and $H_2S_2^+$ were measured again in an experimental arrangement without differential pumping. This was achieved by removing the skimmer and placing the nozzle in the photoionization chamber. The distance between the nozzle and the photoionization center was shortened to approximately 2 cm instead of ~4.5 cm when differential pumping is maintained. In this experimental arrangement, the background H_2S pressure in the photoionization chamber is slightly less than 10^{-4} torr at $P_0 \approx 250$ torr. The signals for S_2^+, HS_2^+, and $H_2S_2^+$ were found to be more than 20 times higher than the observed signals with the differential pumping arrangement. The relative intensities for S_2^+, HS_2^+, and $H_2S_2^+$ measured at ~810 Å were 1:0.35:0.16, respectively.

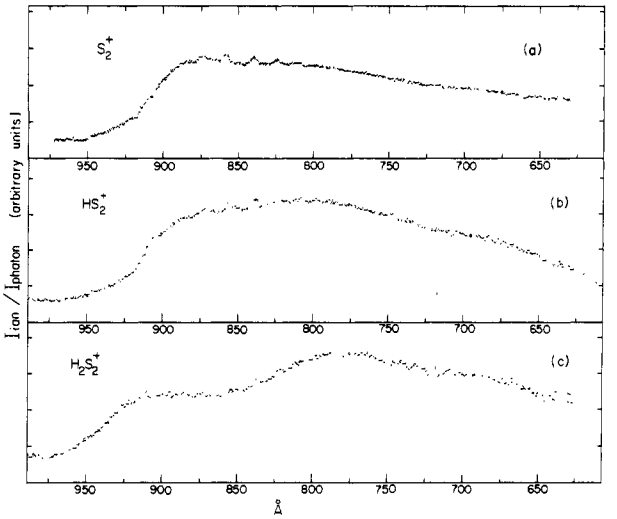

Figure 6. PIE curves for (a) S_2^+, (b) HS_2^+, and (c) $H_2S_2^+$ in the region ~600–990 Å obtained without the differential pumping arrangement [experimental conditions: $P_0 \approx 250$ torr; $T_0 \approx 230$ K; wavelength resolution = 1.4 Å (FWHM)].

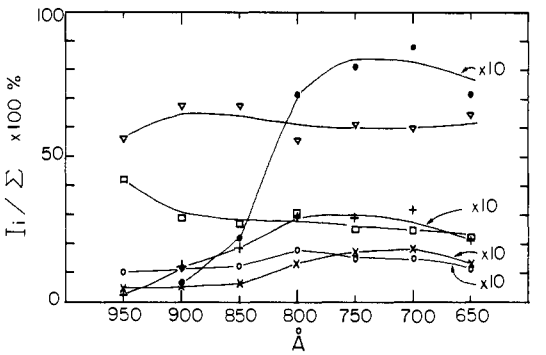

Figure 7. Variations of the relative abundances for $(H_2S)_2^+$ (□), $H_3S_2^+$ (○), H_3S^+ (▽), $H_2S_2^+$ (×), HS_2^+ (●), and S_2^+ (+) as a function of the photon energy; $\sum$ is the sum of $I[(H_2S)_2^+]$, $I(H_3S_2^+)$, $I(H_3S^+)$, $I(H_2S_2^+)$, $I(HS_2^+)$, and $I(S_2^+)$, where $I[(H_2S)_2^+]$, $I(H_3S_2^+)$, $I(H_3S^+)$, $I(H_2S_2^+)$, $I(HS_2^+)$, and $I(S_2^+)$ represent the intensities for $(H_2S)_2^+$, $H_3S_2^+$, H_3S^+, $H_2S_2^+$, HS_2^+, and S_2^+, respectively, after the corrections for isotopic contributions. $I_i = I[(H_2S)_2^+]$, $I(H_3S_2^+)$, $I(H_3S^+)$, $I(H_2S_2^+)$, $I(HS_2^+)$, or $I(S_2^+)$ [experimental conditions: $P_0 \approx 200$ torr; $T_0 \approx 230$ K; wavelength resolution = 1.4 Å (FWHM)].

Parts a, b, and c of Figure 6 show the PIE spectra for S_2^+, HS_2^+, and $H_2S_2^+$ in the region 600–975 Å obtained at $P_0 \approx 250$ torr and $T_0 \approx 230$ K without the differential pumping arrangement. The PIE spectrum for S_2^+ shown in Figure 6a is found to be nearly identical with that for S^+,[14] indicating that the secondary reaction 22 is mainly responsible for the formation of S_2^+. The PIE curve for HS_2^+ shown in Figure 6b is also similar to the S^+ spectrum.[14] The hump starting at approximately 875 Å, which is close to the AE for HS^+ from H_2S, is likely to arise from the reaction $HS^+ + H_2S$. Thus, we conclude that HS_2^+ can be formed by reactions 20 and 23, a conclusion consistent with previous studies.[3,5,6] The ratio of the intensities for S_2^+ and HS_2^+ at 875 Å, which is below the AE for HS^+ from H_2S, is measured to be 3.3. This value is also found to be in excellent agreement with previous reported vaues of 3.2[3] and 3.8.[6] The observed intensity for $H_2S_2^+$ at 875 Å, before corrections for the isotopic contributions, is only ~11% that of S_2^+. Therefore, the finite PIEs observed in Figure 5c at wavelengths longer than ~875 Å are almost totally due to $H^{33}S^{32}S^+$ and $^{34}S^{32}S^+$. The further increase in PIE of $H_2S_2^+$ at wavelengths shorter than 870 Å can be attributed to reaction 21. In short, the above comparison shows that the formation of S_2^+, HS_2^+, and $H_3S_2^+$ by secondary reactions 20–23 have much greater

cross sections than the corresponding reactions by $H_2S^+ + H_2S$. Moreover, the substantial differences observed between the spectra of S_2^+, HS_2^+, and $H_2S_2^+$ shown in Figure 5 and those in Figure 6 support the conclusion that reactions 20–23 contribute little to the spectra observed in Figure 5. The above investigation also demonstrates the importance of using the differential pumping arrangement for the study of unimolecular decompositions of dimer and cluster ions such as reactions 1–6.

The adiabatic IEs for the $\tilde{A}^2A_1$ and $\tilde{B}^2B_2$ states of H_2S^+ obtained by photoelectron spectroscopy[30] are 12.777 eV (970 Å) and 14.643 eV (847 Å), respectively. The AEs for the S_2^+, $H_2S_2^+$, and $H_3S_2^+$ ions are found to be close to the IE of the $\tilde{A}^2A_1$ state. As the photon energy increases to approximately the IE of the $\tilde{B}^2B_2$ state, the PIE curves for the S_2^+, HS_2^+, $H_2S_2^+$, and $H_3S_2^+$ all exhibit further increases in PIE. Qualitatively, one may conclude that reactions 1–5 proceed with higher probabilities when the H_2S^+ moiety in $H_2S^+ \cdot H_2S$ is prepared in the $\tilde{A}^2A_1$ and $\tilde{B}^2B_2$ states than when H_2S^+ is formed in the $\tilde{X}^2B_1$ state. Furthermore, since the productions of S^+ and HS^+ are believed to arise from fast predissociation of H_2S^+, it is likely that many of the fragmentation reactions might be stepwise processes such as

$$H_2S^+ \cdot H_2S \rightarrow S^+ \cdot H_2S + H_2 \rightarrow S_2^+ + 2H_2 \quad (24)$$

$$\rightarrow S^+ \cdot H_2S + H_2 \rightarrow HS_2^+ + H_2 + H \quad (25)$$

$$\rightarrow HS^+ \cdot H_2S + H \rightarrow HS_2^+ + H_2 + H \quad (26)$$

$$\rightarrow HS^+ \cdot H_2S + H \rightarrow H_2S_2^+ + 2H \quad (27)$$

In order to measure the relative reaction probabilities of reactions 1–5 as a function of ionizing photon energy without the interference of processes such as reactions 14–18, it is necessary to operate the H_2S nozzle beam under conditions that minimize the formation of hydrogen sulfide trimers and higher clusters. The intensities for $(H_2S)_2^+$, $H_3S_2^+$, H_3S^+, $H_2S_2^+$, HS_2^+, and S_2^+ were measured at $P_0 \approx 200$ torr and $T_0 \approx 230$ K at wavelength intervals of 50 Å in the region 650–950 Å. Under these beam conditions, the intensities of $H_5S_2^+$, $(H_2S)_3^+$, and higher hydrogen sulfide cluster ions were all found to be within the noise level, indicating that the concentrations of $(H_2S)_n$, $n \geq 3$, were negligible. After careful corrections for isotopic contributions, the true intensities for $(H_2S)_2^+$, $H_3S_2^+$, H_3S^+, $H_2S_2^+$, HS_2^+, and S_2^+, were obtained. The differences in transmission of these ions through the mass spectrometer used in this experiment have not been corrected for. Since the masses of these ions with the exception of H_3S^+ differ only by a few mass units, the transmission factors are expected to have minor effects on the measured relative intensities of $(H_2S)_2^+$, $H_3S_2^+$, $H_2S_2^+$, HS_2^+, and S_2^+. The relative abundances, $I[(H_2S)_2^+]/\sum$, $I(H_3S_2^+)/\sum$, $I(H_3S^+)/\sum$, $I(H_2S_2^+)/\sum$, $I(HS_2^+)/\sum$, and $I(S_2^+)/\sum$ for $(H_2S)_2^+$, $H_3S_2^+$, H_3S^+, $H_2S_2^+$, HS_2^+, and S_2^+, respectively, in percentage as a function of photon energy in the region 650–950 Å are plotted in Figure 7. Here $I[(H_2S)_2^+]$, $I(H_3S_2^+)$, $I(H_3S^+)$, $I(H_2S_2^+)$, $I(HS_2^+)$, and $I(S_2^+)$ represent the true intensities of $(H_2S)_2^+$, $H_3S_2^+$, H_3S^+, $H_2S_2^+$, HS_2^+, and S_2^+, respectively, and $\sum$ is the sum of $I[(H_2S)_2^+]$, $I(H_3S_2^+)$, $I(H_3S^+)$, $I(H_2S_2^+)$, $I(HS_2^+)$, and $I(S_2^+)$. As shown in Figure 7, $H_3S^+ + HS$ is found to be the dominate product channel with only minor variation in fragmentation probability in this region. This analysis also confirms the above conclusions that the $S_2^+ + 2H_2$, $HS_2^+ + H_2 + H$, $H_2S_2^+ + H_2$, and $H_3S_2^+ + H$ are weak product channels that have higher reaction probabilities when H_2S^+ in $H_2S^+ \cdot H_2S$ is formed in the $\tilde{A}^2A_1$ or $\tilde{B}^2B_2$ states.

In summary, the study of the unimolecular decomposition of $(H_2S)_2^+$ using the molecular beam photoionization method has allowed the unambiguous identification of the S_2^+, HS_2^+, $H_2S_2^+$, H_3S^+, and $H_3S_2^+$ ions to be the primary product ions from the reactions of $H_2S^+ + H_2S$. From the AE and IE measurements of various ions, the energetics of HS_2^+, $H_3S_2^+$, $H_5S_2^+$, H_3S^+, $(H_2S)_2^+$, and $(H_2S)_3^+$ have been calculated. This study also reveals that the ion–molecule reactions between H_2S^+ and H_2S to form S_2^+, HS_2^+, $H_2S_2^+$, and $H_3S_2^+$ are strongly favored for H_2S^+ in the $\tilde{A}^2A_1$ and $\tilde{B}^2B_2$ states in comparison to the $\tilde{X}^2B_1$ state. Furthermore, the decompositions of the $H_2S^+ \cdot H_2S$ complexes to form S_2^+, HS_2^+, and $H_2S_2^+$ are likely to proceed by stepwise processes as shown in reactions 24–27.

Acknowledgment. We thank Dr. Y. Ono and Dr. S. H. Linn for their assistance in obtaining part of the data of this experiment.

Registry No. $H_5S_2^+$, 62873-60-3; $H_3S_2^+$, 68941-81-1; $H_2S_2^+$, 63228-83-1; HS_2^+, 63228-82-0; S_2^+, 12597-02-3; H_3S^+, 18155-21-0; H_2S, 7783-06-4; H_2S^+, 26453-60-1; H, 12385-13-6; H_2, 1333-74-0.

Analysis of Fully Anisotropic Overall Molecular Tumbling with Group Internal Rotation: Steroid Examples

George C. Levy,* Anil Kumar, and Dehua Wang

Contribution from the N.I.H. Resource for Multi-Nuclei NMR and Data Processing, Chemistry Department, Syracuse University, Syracuse, New York 13210. *Received April 5, 1983*

Abstract: The theory for fully anisotropic overall motion with internal rotation is presented and applied to substituted 5α-androstane steroids to compute the diffusion constants for overall motion as well as internal CH_3 rotations. It is found that calculations give close fits with the experimental data. Although existing literature discusses steroid motion in terms of isotropic or axially symmetric motion, it was found in all cases that the androstane skeletons reorient anisotropically. In two of six compounds studied, overall motion was close to axially symmetric; in the remaining molecules the three diffusion constants were significantly different. Calculations of rotational rates for the C-18 and C-19 methyl groups showed relatively fast spinning of C-19.

Carbon-13 spin–lattice relaxation times (T_1) have been widely used to investigate details of molecular motion in solution.[1-4] A rigid molecule that is not spherically symmetric will generally undergo anisotropic rotation.[1-7] The anisotropy of rotation can arise from inertial differences and because the asymmetric (often assumed ellipsoidal) shape of the molecule has variable requirements for reorientation within the solvent "cage" (e.g., solvent molecules must be translated for motions about axes perpendicular

(1) Wright, D. A.; Axelson, D. E.; Levy, G. C. In "Topics in Carbon-13 NMR Spectroscopy"; Levy, G. C., Ed.; Wiley-Interscience: New York, 1979; Vol. 3, Chapter 2, and references cited therein.
(2) Komoroski, R. A.; Levy, G. C. *J. Phys. Chem.* **1976**, *80*, 2414.
(3) Howarth, O. W. *J. Chem. Soc., Perkin Trans. 2* **1982**, 263.
(4) Levy, G. C.; Cargioli, J. D.; Anet, F. A. L. *J. Am. Chem. Soc.* **1973**, *95*, 1528.
(5) Beierbeck, H.; Martino, R.; Saunders, J. K. *Can. J. Chem.* **1980**, *58*, 102.
(6) (a) Axelson, D. E.; Holloway, C. E. *Can. J. Chem.* **1980**, *58*, 679. (b) Somorjai, R. L.; Deslauriers, R. *J. Am. Chem. Soc.* **1976**, *98*, 6460.
(7) Levy, G. C.; Craik, D. J.; Phan Viet, M. T.; Dekmezian, A. *J. Am. Chem. Soc.* **1982**, *104*, 25.

0002-7863/83/1505-7536$01.50/0